IOPscience iopscience.iop.org

Home Search Collections Journals About Contact us My IOPscience

Shockley-type surface states on low-index faces of Cu-based alloys with polyvalent solutes

This article has been downloaded from IOPscience. Please scroll down to see the full text article.

1991 J. Phys.: Condens. Matter 3 801

(http://iopscience.iop.org/0953-8984/3/7/005)

View the table of contents for this issue, or go to the journal homepage for more

Download details:
IP Address: 171.66.16.151
The article was downloaded on 11/05/2010 at 07:06

Please note that terms and conditions apply.

J. Phys.: Condens. Matter 3 (1991) 801–812. Printed in the UK

Shockley-type surface states on low-index faces of Cu-based alloys with polyvalent solutes

R Prasad†, A Y Serageldin and A Bansil
Department of Physics, Northeastern University, Boston, MA 02115, USA

Received 23 August 1990

Abstract. We consider Shockley-type surface states (SSS) in substitutionally disordered alloys. For this purpose the Green function for the semi-infinite system is obtained by matching the bulk Korringa–Kohn–Rostoker coherent potential approximation (KKR-CPA) Green function with the free-electron Green function on the bounding surface. The formalism is applied to calculate binding energies and disorder induced smearings of the $\bar{Y}$-centred SSS on the (110) surface and the $\bar{\Gamma}$- centred SSS on the (111) surfaces of Cu, $Cu_{90}Al_{10}$, $Cu_{70}Zn_{30}$, and $Cu_{90}Ge_{10}$. Our theoretical predictions with regard to changes in the binding energy and the disorder induced smearing in $Cu_{90}Al_{10}$ where corresponding angle-resolved photoemission experiments are available for comparison are in reasonable accord with measurements. Our computations indicate that the binding energy of the SSS in Cu-based alloys will generally increase with increasing electron/atom (e/a) ratio.

1. Introduction

Although the bulk electronic structure of disordered alloys has been studied extensively in recent years, relatively little work exists concerning their surface electronic structure. As is well known, the presence of the surface can induce substantial changes in electronic structure, causing in particular the appearance of new types of states localized in the surface region; such surface states have in fact been observed in angle-resolved photoemission experiments in a number of alloys (Pessa *et al* 1981, Asonen *et al* 1982, Jordan and Sohal 1982, Rao *et al* 1984, Asonen *et al* 1985, Heimann *et al* 1981; for a review see Bansil and Pessa 1983, Jordan and Durham 1989.) In this article, we consider one class of surface states, namely the Shockley surface states (SSS), associated with the semi-infinite surface of a disordered alloy. (For a general review see, e.g., Inglesfield (1982).) Specific results for the low-index faces of Cu and Cu-based solid solutions with polyvalent impurities Zn, Al, and Ge are presented and discussed.

Our formal approach is to employ the Green function matching method used extensively by Inglesfield and co-workers (Inglesfield (1982) and references therein; for a general discussion of the method see Garcia-Moliner and Flores (1979)) in a number of surface related problems, to construct the average Green function for the semi-infinite alloy by matching the vacuum and bulk Green functions on the bounding surface. The bulk Green function is obtained on the basis of the Korringa–Kohn–Rostoker

† Permanent address: Physics Department, Indian Institute of Technology, Kanpur, India.

coherent potential approximation (KKR-CPA) scheme for treating a randomly disordered alloy. (For a review and further references see: Bansil 1987, Stocks and Winter 1984, Ehrenreich and Schwartz 1976.) The presence of the surface is modelled as an abrupt potential step. These approximations obviously imply a rather idealized model of a surface. Nevertheless, such an approach has yielded reasonable results in describing aspects of the surface electronic structure in several cases of pure metals and disordered alloys. (See reviews by Inglesfield 1982, Jordan and Durham 1989.)

Concerning related work, the Green function matching of the sort invoked in the present study is presumably implicit in the formalism of Durham and co-workers (Durham 1984) who have considered angle-resolved photoemission intensities in disordered alloys based on the one-step model of Pendry (1976); these authors have in particular calculated SSS in CuNi(111) and CuPd(111) binary alloys (Jordan and Durham 1989). We note also some tight-binding model Hamiltonian work in connection with surface states in alloys. (Berk 1975, Ishida *et al* 1976, Velicky and Kudrnosky 1977, Wysokinski *et al* 1980, Bullet 1982.)

An outline of this article is as follows. These introductory remarks are followed in section 2 by a summary of the formalism used. Only the briefest presentation of the formalism is given in order to enable us to state clearly the approximations invoked and the equations used in the computations; the general aspects of the Green function matching method and the multiple scattering theory techniques have been described extensively in the literature. An explicit secular equation for the SSS-bands in a disordered alloy is derived. Section 3 gives details of muffin-tin potentials and other model parameters used in the calculations, and presents and discusses the binding energies and disorder induced smearings of the $\bar{Y}$-centred SSS on (110) surface and the $\bar{\Gamma}$-centred SSS on the (111) surface of Cu and Cu-based solid solution $Cu_{90}Al_{10}$, $Cu_{70}Zn_{30}$, and $Cu_{90}Ge_{10}$. The theoretical predictions are compared with the measurements in $Cu_{90}Al_{10}$ where corresponding angle-resolved photoemission results are available†. The concluding discussion in section 4 comments further on the limitations of our model, and gives a summary of our results.

2. Theoretical formulation

2.1. General equations

An outline of the Green function matching approach (Inglesfield 1982) is as follows. Consider two regions I and II, with potentials $V_{\rm I}$ and $V_{\rm II}$ respectively, separated by the surface S. The Green functions $G_{\rm I}$ and $G_{\rm II}$ for the two regions are given by the equations

$$(-\nabla^2 + V_{\rm I}(\boldsymbol{r}) - E)G_{\rm I}(\boldsymbol{r},\boldsymbol{r}') = -\delta(\boldsymbol{r},\boldsymbol{r}') \tag{1}$$

$$(-\nabla^2 + V_{\rm II}(\boldsymbol{r}) - E)G_{\rm II}(\boldsymbol{r},\boldsymbol{r}') = -\delta(\boldsymbol{r},\boldsymbol{r}')\,. \tag{2}$$

The Green function G for the combined system I + II satisfies

$$(-\nabla^2 + V(\boldsymbol{r}) - E)G(\boldsymbol{r},\boldsymbol{r}') = -\delta(\boldsymbol{r},\boldsymbol{r}') \tag{3}$$

† The present $Cu_{90}Al_{10}$ alloy results were presented by Serageldin *et al* (1990).

where $V = V_{\mathrm{I}}$ when $\boldsymbol{r}$ is in region I, and $V = V_{\mathrm{II}}$ when $\boldsymbol{r}$ is in region II. Multiplying equation (3) by G_{I} and (1) by G, subtracting, and integrating over the volume of region I, upon using Green's theorem yields

$$G(\boldsymbol{r},\boldsymbol{r}') = G_{\mathrm{I}}(\boldsymbol{r},\boldsymbol{r}_s) - \int_S \mathrm{d}^2\boldsymbol{r}_s \left(G_{\mathrm{I}}(\boldsymbol{r},\boldsymbol{r}_s)\frac{\partial G(\boldsymbol{r}_s,\boldsymbol{r}')}{\partial n_s} - \frac{\partial G_{\mathrm{I}}(\boldsymbol{r},\boldsymbol{r}_s)}{\partial n_s} G(\boldsymbol{r}_s,\boldsymbol{r}') \right) \tag{4}$$

for $\boldsymbol{r}$, $\boldsymbol{r}'$ in region I, and

$$G(\boldsymbol{r},\boldsymbol{r}') = \int_S \mathrm{d}^2\boldsymbol{r}_s \left(G_{\mathrm{II}}(\boldsymbol{r},\boldsymbol{r}_s)\frac{\partial G(\boldsymbol{r}_s,\boldsymbol{r}')}{\partial n_s} - \frac{\partial G_{\mathrm{II}}(\boldsymbol{r},\boldsymbol{r}_s)}{\partial n_s} G(\boldsymbol{r}_s,\boldsymbol{r}') \right) \tag{5}$$

for $\boldsymbol{r}$ in region II and $\boldsymbol{r}'$ in region I. Here $\partial/\partial n_s$ denotes the normal derivative outward from I. Setting $\boldsymbol{r} = \boldsymbol{r}_s$ in equations (4) and (5) yields two simultaneous equations that can be solved for the surface values $G(\boldsymbol{r}_s,\boldsymbol{r}')$ and $\partial G(\boldsymbol{r}_s,\boldsymbol{r}')/\partial n_s$ by expanding these quantities in terms of an appropriate complete set of functions. $G(\boldsymbol{r},\boldsymbol{r}')$ is then determined uniquely for all $\boldsymbol{r}$ and $\boldsymbol{r}'$ from the surface values of G via equations (4) and (5).

2.2. Bulk alloy and free-electron Green functions

In order to treat the ideal semi-infinite surface of a disordered alloy, we take G_{I} to be the bulk KKR-CPA Green function G_a, and G_{II} to be the free electron Green function G_0. For simplicity, the bulk alloy potential is assumed to extend right up to the surface, where it abruptly changes to the vacuum potential with the step V_0. The relevant form of G_a for the random binary alloy $\mathrm{A}_x\mathrm{B}_y$ (with $y \equiv 1 - x$) of non-overlapping muffin-tin potentials (radius R_m) is well known (see Stocks and Winter 1984, Bansil 1987) and may be written in terms of the regular and irregular solutions $R_l^{A(B)}$ and $\tilde{R}_l^{A(B)}$ of the radial Schrödinger equation in the A(B) muffin-tin sphere, normalized such that outside the muffin-tin sphere (i.e. for $r \geq R_m$)

$$R_l^{\mathrm{A(B)}}(r) = \eta_l(\kappa r) - \cot\delta_l^{\mathrm{A(B)}} j_l(\kappa r) \tag{6a}$$

$$\tilde{R}_l^{\mathrm{A(B)}}(r) = j_l(\kappa r)\,. \tag{6b}$$

Here $\delta_l^{\mathrm{A(B)}}$ are the phase-shifts associated with the A(B) potential evaluated at energy E and $\kappa \equiv \sqrt{E}$. η_l and j_l are the spherical Neumann and Bessel functions respectively. The Green function $G_a^{nn}(\boldsymbol{r},\boldsymbol{r}')$ when $\boldsymbol{r}$ and $\boldsymbol{r}'$ both lie in the nth cell is given by

$$G_a^{nn}(\boldsymbol{r},\boldsymbol{r}') = \kappa \sum_L Y_L(\hat{r}) \sum_i c_i [\kappa R_l^i(r) C_L^i R_l^i(r') - R_l^i(r)\tilde{R}_l^i(r')] Y_L(\hat{r}')\,. \tag{7}$$

The index i runs over atomic species, with $c_{\mathrm{A}} = x$ and $c_{\mathrm{B}} = y$. $Y_L(\hat{r})$ are real spherical harmonics, and

$$C_L^{\mathrm{A(B)}} = -D_L^{\mathrm{A(B)}} T_{LL}^{00} \tag{8}$$

where

$$D_L^{\mathrm{A(B)}} = \{1 + [(\tau_l^{\mathrm{A(B)}})^{-1} - (\tau_L^{\mathrm{CPA}})^{-1}] T_{LL}^{00}\}^{-1}\,. \tag{9}$$

Here $T^{nm}_{LL'}$ are the energy-shell matrix elements of the KKR-CPA path operator, $\tau_l^{A(B)}$ and τ_L^{CPA} are on the energy-shell matrix elements of the t-matrices for atom A(B) and the CPA effective atom, respectively. The Green function $G_a^{nm}(\boldsymbol{r},\boldsymbol{r}')$ for the case when $\boldsymbol{r}$ and $\boldsymbol{r}'$ are in different unit cells, with $\boldsymbol{r}$ lying in the nth cell and $\boldsymbol{r}'$ in the mth cell is given by

$$G_a^{nm}(\boldsymbol{r},\boldsymbol{r}') = \kappa^2 \sum_{LL'} Y_L(\hat{r}) \Big(\sum_{ij} c_i c_j R_l^i(r) P_{LL'}^{ij}(n-m) R_l^j(r') \Big) Y_{L'}(\hat{r}') \tag{10}$$

where

$$P_{LL'}^{ij}(n-m) = D_L^i T_{LL'}^{nm} D_{L'}^j. \tag{11}$$

The symmetry of the semi-infinite system can be exploited by considering suitable periodic Green functions, rather than the functions G_a and G_0. For this purpose we define partial Fourier transforms $\tilde{G}_{aK}$ and $\tilde{G}_{0K}$ for a wavevector $\boldsymbol{K}$ parallel to the surface Brillouin zone (SBZ), where

$$\tilde{G}_{aK}(\boldsymbol{r},\boldsymbol{r}') = \sum_m G_a(\boldsymbol{r},\boldsymbol{r}' - \boldsymbol{R}_m^s) \exp(-\mathrm{i}\boldsymbol{K}\cdot\boldsymbol{R}_m^s) \tag{12}$$

with a similar expression for $\tilde{G}_{0K}$. Here the summation extends over the N_s vectors $\{\boldsymbol{R}_m^s\}$ of the surface lattice. $\tilde{G}_{aK}$ can be expressed in terms of the Fourier transform

$$\hat{G}_{ak}(\boldsymbol{r},\boldsymbol{r}') = \sum_m G_a(\boldsymbol{r},\boldsymbol{r}' - \boldsymbol{R}_m) \exp(-\mathrm{i}\boldsymbol{k}\cdot\boldsymbol{R}_m) \tag{13}$$

of the bulk Green function, where the sum runs over the N lattice points $\{\boldsymbol{R}_m\}$, and $\boldsymbol{k}$ is a Bloch waveector. The relation between $\tilde{G}_{aK}$ and $\hat{G}_{ak}$ is

$$\tilde{G}_{aK}(\boldsymbol{r},\boldsymbol{r}') = \frac{d}{2\pi} \int_{-\pi/d}^{\pi/d} \mathrm{d}k_\perp \, \hat{G}_{a(K,k_\perp)}(\boldsymbol{r},\boldsymbol{r}') \tag{14}$$

where d is the interplanar distance; K and $k_\perp$ are the parallel and normal components of $\boldsymbol{k}$ respectively.

We now introduce the angular momentum representation

$$\tilde{G}_{aK}(\boldsymbol{r},\boldsymbol{r}') = \sum_{LL'} \tilde{\mathcal{G}}_{aK,LL'}(r,r') Y_L(\hat{r}) Y_{L'}(\hat{r}') . \tag{15}$$

An explicit formula for the coefficients $\tilde{\mathcal{G}}_{aK,LL'}$ is obtained straightforwardly by using equations (7)–(14). The results is

$$\begin{aligned}\tilde{\mathcal{G}}_{aK,LL'}(r,r') = {} & \Big(\kappa \sum_i c_i [\kappa R_l^i(r) \mathcal{C}_L^i R_l^i(r') - R_l^i(r) \tilde{R}_l^i(r')] \delta_{LL'} \Big) \\ & + \kappa^2 \sum_{ij} c_i c_j R_l^i(r) \tilde{P}_{LL'}^{ij}(\boldsymbol{K}) R_l^j(r') \end{aligned} \tag{16}$$

where we have defined

$$\tilde{P}^{ij}_{LL'}(K) = D^{i}_{L}\left(\frac{d}{\pi}\int_{-\pi/d}^{\pi/d} \mathrm{d}k_{\perp}\, \Gamma^{\mathrm{CPA}}_{LL'}(E;\boldsymbol{K},\boldsymbol{k}_{\perp})\right) D^{j}_{L'} \tag{17}$$

$$\begin{aligned}\Gamma^{\mathrm{CPA}}_{LL'}(E,\boldsymbol{k}) &= \sum_{m\neq 0} T^{0m}_{LL'} \exp(-\mathrm{i}\boldsymbol{k}\cdot\boldsymbol{R}_m) + T^{00}_{LL'}\delta_{LL'} \\ &= [(\tau^{\mathrm{CPA}}_{L})^{-1}\delta_{LL'} - B(\boldsymbol{k},E)_{LL'}]^{-1} + T^{00}_{LL'}\delta_{LL'}.\end{aligned} \tag{18}$$

Here $B(\boldsymbol{k},E)$ is the matrix of the familiar KKR structure constants. The angular momentum decomposition of the free electron Green function $\tilde{G}_{0\boldsymbol{K}}(\boldsymbol{r},\boldsymbol{r}')$ is obtained similarly. Thus we have

$$\tilde{G}_{0\boldsymbol{K}}(\boldsymbol{r},\boldsymbol{r}') = \sum_{LL'} \tilde{\mathcal{G}}_{0\boldsymbol{K},LL'}(r,r') Y_L(\hat{r}) Y_{L'}(\hat{r}') \tag{19}$$

with

$$\tilde{\mathcal{G}}_{0\boldsymbol{K},LL'}(r,r') = -\gamma j_l(\mathrm{i}\gamma r_<) h^{(1)}_l(\mathrm{i}\gamma r_>)\delta_{LL'} + \mathcal{D}^{L''}_{LL'} j_l(\mathrm{i}\gamma r) j_{l'}(\mathrm{i}\gamma r') \tag{20}$$

where

$$\mathcal{D}^{L''}_{LL'} = 4\pi \mathrm{i}^{l-l'} \sum_{L''} \mathrm{i}^{-l''} \mathcal{N}^{L''}_{LL'} [-\gamma \sum_{j} h_{l''}(i\gamma R^{s}_{j}) \exp(\mathrm{i}\boldsymbol{K}\cdot\boldsymbol{R}^{s}_{j}) Y_{L''}(\hat{R}_j)] \tag{21}$$

with $\gamma^2 = V_0 - E$. $-\gamma^2$ is the electron energy with respect to the vacuum zero and

$$\mathcal{N}^{L''}_{LL'} = \int \mathrm{d}\Omega\, Y_L(\Omega) Y_{L'}(\Omega) Y_{L''}(\Omega) \tag{22}$$

are the Gaunt numbers.

The implementation of the preceding formalism is simplified if one uses Green functions $\tilde{G}^{\mathrm{WS}}_{a\boldsymbol{K}}$ and $\tilde{G}^{\mathrm{WS}}_{o\boldsymbol{K}}$ (rather than $\tilde{G}_{a\boldsymbol{K}}$ and $\tilde{G}_{0\boldsymbol{K}}$) which satisfy Neumann-type boundary conditions at the matching surface, i.e.

$$\frac{\partial \tilde{G}^{\mathrm{WS}}_{a\boldsymbol{K}}}{\partial n_s} = \frac{\partial \tilde{G}^{\mathrm{WS}}_{o\boldsymbol{K}}}{\partial n_s} = 0. \tag{23}$$

Such Green functions are easily constructed from $\tilde{G}_{a\boldsymbol{K}}$ and $\tilde{G}_{0\boldsymbol{K}}$ and their derivatives. The spherical harmonic expansions for $\tilde{G}^{\mathrm{WS}}_{a\boldsymbol{K}}$ and $\tilde{G}^{\mathrm{WS}}_{0\boldsymbol{K}}$ are given by

$$\tilde{\mathcal{G}}^{\mathrm{WS}}_{a\boldsymbol{K}} = (1 - R_s^2 \tilde{\mathcal{G}}'_{a\boldsymbol{K}} M)^{-1} \tilde{\mathcal{G}}_{a\boldsymbol{K}} \tag{24}$$

$$\tilde{\mathcal{G}}^{\mathrm{WS}}_{o\boldsymbol{K}} = (1 + R_s^2 \tilde{\mathcal{G}}'_{o\boldsymbol{K}} M)^{-1} \tilde{\mathcal{G}}_{o\boldsymbol{K}} \tag{25}$$

where $\tilde{\mathcal{G}}_{a\boldsymbol{K}}$ and $\tilde{\mathcal{G}}_{0\boldsymbol{K}}$ are the spherical harmonics expansions of $\tilde{G}_{a\boldsymbol{K}}$ and $\tilde{G}_{0\boldsymbol{K}}$ respectively over a WS sphere of radius R_s, $\tilde{\mathcal{G}}'_{a\boldsymbol{K}}$ and $\tilde{\mathcal{G}}'_{0\boldsymbol{K}}$ are the corresponding derivatives, and

$$M_{LL'} = \int_S Y_L(\hat{R}_s) Y_{L'}(\hat{R}_s)\, \mathrm{d}\Omega \tag{26}$$

is a matrix which involves an integral of the spherical harmonics over the matching surface S.

2.3. Green function for the semi-infinite alloy surface

The Green function $\tilde{G}_K(\boldsymbol{r},\boldsymbol{r}')$ for the combined system (defined in a manner analogous to equation (12)) can be obtained in terms of $\tilde{G}_{aK}^{\mathrm{WS}}$ and $\tilde{G}_{0K}^{\mathrm{WS}}$ by using the matching conditions (4) and (5). Hereafter, following Inglesfield (1978; such an approximation is commonly invoked in the theory of muffin-tin systems) we will approximate the unit cell by a Wigner-Seitz (WS) sphere. The matching surface then becomes part of the WS sphere surface in the shape of a spherical 'cap'. We thus have

$$\tilde{G}_K(\boldsymbol{r},\boldsymbol{r}') = \tilde{G}_{aK}^{\mathrm{WS}}(\boldsymbol{r},\boldsymbol{r}') - \int_S \mathrm{d}^2\boldsymbol{r}_s\, \tilde{G}_{aK}^{\mathrm{WS}}(\boldsymbol{r},\boldsymbol{r}_s)\frac{\partial \tilde{G}_K(\boldsymbol{r}_s,\boldsymbol{r}')}{\partial n_s} \tag{27}$$

for $\boldsymbol{r}$ and $\boldsymbol{r}'$ inside the WS sphere, and

$$\tilde{G}_K(\boldsymbol{r},\boldsymbol{r}') = \int_S \mathrm{d}^2\boldsymbol{r}_s\, \tilde{G}_{oK}^{\mathrm{WS}}(\boldsymbol{r},\boldsymbol{r}_s')\frac{\partial \tilde{G}_K(\boldsymbol{r}_s,\boldsymbol{r}')}{\partial n_s} \tag{28}$$

when $\boldsymbol{r}'$ lies in the alloy and $\boldsymbol{r}$ in the vacuum. Using spherical harmonic expansions for $\tilde{G}_K$, $\tilde{G}_a^{\mathrm{WS}}$, and $\tilde{G}_0^{\mathrm{WS}}$, and putting $r = R_s$ in equations (27) and (28), we get

$$\tilde{\mathcal{G}}_{K,LL'}(R_s,r') = \tilde{\mathcal{G}}_{aK,LL'}^{\mathrm{WS}}(R_s,r') - R_s^2 \sum_{L''L'''} \tilde{\mathcal{G}}_{aK,LL''}^{\mathrm{WS}}(R_s,R_s) M_{L''L'''} \tilde{\mathcal{G}}'_{K,L'''L'}(R_s,r') \tag{29}$$

$$\tilde{\mathcal{G}}_{K,LL'}(R_s,r') = R_s^2 \sum_{L''L'''} \tilde{\mathcal{G}}_{0K,LL''}^{\mathrm{WS}}(R_s,R_s) M_{L''L'''} \tilde{\mathcal{G}}'_{K,L'''L'}(R_s,r'). \tag{30}$$

Equations (29) and (30) may be written in a compact matrix notation as

$$\tilde{\mathcal{G}}_K = \tilde{\mathcal{G}}_{aK}^{\mathrm{WS}} - R_s^2 \tilde{\mathcal{G}}_{aK}^{\mathrm{WS}} M \tilde{\mathcal{G}}'_K \tag{31a}$$

$$\tilde{\mathcal{G}}_K = R_s^2 \tilde{\mathcal{G}}_{0K}^{\mathrm{WS}} M \tilde{\mathcal{G}}'_K\,. \tag{31b}$$

Solving for the derivative, we obtain

$$\tilde{\mathcal{G}}'_K = (R_s^2 M)^{-1}[\tilde{\mathcal{G}}_{0K}^{\mathrm{WS}} + \tilde{\mathcal{G}}_{aK}^{\mathrm{WS}})]^{-1}\tilde{\mathcal{G}}_{aK}^{\mathrm{WS}}\,. \tag{32}$$

Using (32) in (27), keeping definition (26) in mind, yields

$$\tilde{G}_K(\boldsymbol{r},\boldsymbol{r}') = \tilde{G}_{aK}^{\mathrm{WS}}(\boldsymbol{r},\boldsymbol{r}') - \sum_{LL',L''L'''} \{\tilde{\mathcal{G}}_{aK,LL''}^{\mathrm{WS}}(r,R_s)[\tilde{\mathcal{G}}_{0K}^{\mathrm{WS}}(R_s,R_s)M + \tilde{\mathcal{G}}_{aK}^{\mathrm{WS}}(R_s,R_s)M]^{-1}_{L''L'''}\tilde{\mathcal{G}}_{aK,L'''L'}^{\mathrm{WS}}(R_s,r')Y_L(\hat{r})Y_{L'}(\hat{r}')\} \tag{33}$$

which is the desired expression for the semi-infinite alloy surface Green function in terms of the bulk KKR-CPA and the free electron Green functions.

2.4. Shockley-type surface state bands

The spectral density of states associated with the Green function $\tilde{G}_{\boldsymbol{K}}(\boldsymbol{r},\boldsymbol{r}')$ is

$$\varrho_{s,\boldsymbol{K}}(E) = -\pi^{-1}\int_{\mathrm{WS}} \mathrm{d}^3\boldsymbol{r}\,\mathrm{Im}\,\tilde{G}_{\boldsymbol{K}}(\boldsymbol{r},\boldsymbol{r}) = \varrho_{a\boldsymbol{K}}(E) + \varrho_{b\boldsymbol{K}}(E) \tag{34}$$

with the definitions

$$\varrho_{a\boldsymbol{K}}(E) = -\pi^{-1}\int_{\mathrm{WS}} \mathrm{d}^3\boldsymbol{r}\,\mathrm{Im}\,\tilde{G}^{\mathrm{WS}}_{a\boldsymbol{K}}(\boldsymbol{r},\boldsymbol{r}) \tag{35}$$

$$\varrho_{b\boldsymbol{K}}(E) = \pi^{-1}\sum_{L}\int_{\mathrm{WS}} r^2\,\mathrm{d}r\,\mathrm{Im}\,[(\tilde{\mathcal{G}}^{\mathrm{WS}}_{a\boldsymbol{K}})^2(r,R_s)\{\tilde{\mathcal{G}}^{\mathrm{WS}}_{0\boldsymbol{K}}(R_s,R_s)M + \tilde{\mathcal{G}}^{\mathrm{WS}}_{a\boldsymbol{K}}(R_s,R_s)M\}^{-1}]_{LL}\,. \tag{36}$$

$\varrho_{s\boldsymbol{K}}(E)$ is periodic in the SBZ and is the surface analogue of the Bloch spectral density in a bulk system. An integral of $\varrho_{s\boldsymbol{K}}(E)$ over $\boldsymbol{K}$ yields the density of states. The contribution $\varrho_{a\boldsymbol{K}}(E)$ on the right side of (34) arises from the bulk alloy Green function and gives the projection of the Bloch spectral density on to the SBZ. The second term $\varrho_{b\boldsymbol{K}}(E)$ represents the surface contribution, giving additional peaks in the spectral density whenever

$$\|\tilde{\mathcal{G}}^{\mathrm{WS}}_{\mathrm{surf}}\| \equiv \|\tilde{\mathcal{G}}^{\mathrm{WS}}_{o\boldsymbol{K}} + \tilde{\mathcal{G}}^{\mathrm{WS}}_{a\boldsymbol{K}}\| = 0\,. \tag{37}$$

This is the secular equation for obtaining Shockley state bands for the semi-infinite alloy surface. For a fixed $\boldsymbol{K}$, the roots $E_n(\boldsymbol{K})$ of (37) will be real for a perfect crystal surface. In an alloy, on the other hand, (37) will in general yield 'complex' surface energy bands; the imaginary part of $E_n(\boldsymbol{K})$ represents the disorder scattering of surface states.

3. Results for low-index faces of Cu-based alloys

3.1. Computational details

The Cu, Al, Zn, and Ge muffin-tin potentials used in the present calculations are non-self-consistent and are based on the Herman–Skillman charge densities overlapped on the FCC Cu lattice of lattice constant 6.8309 au via the Mattheiss procedure. The specific muffin-tin potentials used in this work are identical to those employed in our previous studies of CuAl(Asonen *et al* 1982), CuZn (Prasad *et al* 1981), and CuGe (Prasad and Bansil 1982, Bansil *et al* 1984) solid solutions, where they yield a reasonable accord with the corresponding bulk band structures deduced from angle-resolved photoemission and other experiments. In computing the Green function for the semi-infinite surface, the height of the surface step V_0 was chosen to reproduce the measured work function W from the calculated Fermi energy E_{F} using the relation, $V_0 = E_{\mathrm{F}} + W$. In Cu, W for the (110) surface is 4.49 eV, and E_{F} is 8.40 eV, giving $V_0 = 12.9$ eV. The Shockley states discussed in this article were found to be quite insensitive to variations on the order of 0.1 eV in the value of the parameter V_0. Differences in the values of work function between various low-index faces of Cu, and between Cu and Cu-based alloys of present interest are generally less than a few

tenths of an eV, as are the differences in the Fermi energies between Cu and the alloys considered in this work. For this reason, we also used $V_0 = -12.9$ eV in the alloy surface calculations. For the results given below, the matching surface in all cases was taken to be the hemispherical upper portion of the WS sphere (radius 2.67 au). A number of other computations using larger, as well as smaller, values of the effective radius of the matching sphere surface were carried out in order to ascertain the effect of the position of the matching surface on the SSS energy. While the absolute values of the surface states do vary with these changes as expected, the relative shifts in the surface state positions upon alloying, our main focus in this article, were found to be quite insensitive to such variations in the parameters of the model potential.

The present computer codes were checked extensively in the limiting case of a pure metal where they reproduce the detailed results concerning the surface state position and the phase of the surface Green function in Ni(001) given by Inglesfield (1978) for the Wakoh (1965) Ni potential. Care is needed in evaluating the Green function expansion co-efficients $\tilde{\mathcal{G}}_{aKLL'}$ (cf equation (16)) which in view of equations (17)–(18) involve integrals with a singular integrand in the pure-metal limit. We evaluated these integrals by adding a small imaginary part of $\approx 10^{-5}$ Ryd in energy; the accuracy of the results was however checked by test calculations with much smaller imaginary parts of energy. This procedure was also employed in obtaining the path operators T_{00} in Cu. The KKR-CPA scattering phase shifts in $Cu_{90}Al_{10}$, $Cu_{70}Zn_{30}$, and $Cu_{90}Ge_{10}$, and the path operators in Cu as well as the alloy were calculated over a fine (a few mRyd) mesh in energy in order to obtain the complex bulk energy bands in the alloy accurately in the energy region of the surface states.

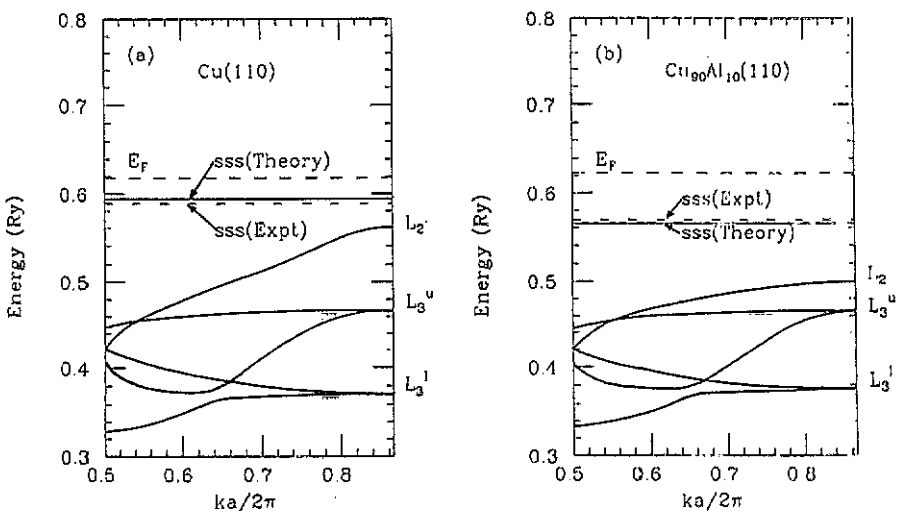

Figure 1. Bulk energy bands along the straight line joining $\boldsymbol{k} = (0, 0, 0.5)2\pi/a$ and the symmetry point L in the Brillouin zone in: (*a*) Cu, and (*b*) $Cu_{90}Al_{10}$, relevant to the $\bar{\Gamma}$-centred Shockley state on the (110) surface. The bands in the alloy are of course complex, but are shown without their disorder induced widths for simplicity. The horizontal lines mark the positions of the Fermi energy E_F (broken line), the experimental values of binding energy of the Shockley surface states SSS (after Asonen *et al* (1982), chain line), and the theoretically predicted SSS binding energies (present work, full line).

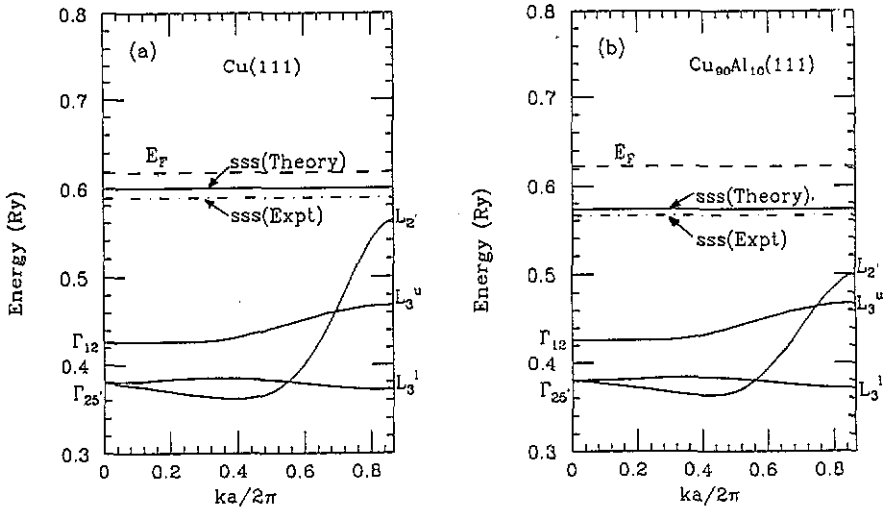

Figure 2. As figure 1 but for the $\bar{\Gamma}$-centred Shockley state on the (111) surface. The relevant bulk bands along the Γ–L symmetry direction are shown.

Our procedure for investigating surface states was as follows. The projected bulk bands at various $\boldsymbol{K}$-points in the SBZ in Cu and the alloys (the energy bands in the disordered alloy are of course complex) were calculated. If a band gap existed in the projected bulk bands, we searched for possible Shockley state solutions of equation (37). Figure 1 is illustrative in this regard for the (110) surface; it shows bulk bands in Cu and $Cu_{90}Al_{10}$ for various $k_\perp$ values for a fixed $K_\parallel$ corresponding to the $\bar{Y}$ point in the SBZ. An sp-like band gap is seen to exist below E_F with an edge at the position of the $L_{2'}$ level in both Cu and $Cu_{90}Al_{10}$. By examining the zeros of the determinant of the surface matrix $\tilde{\mathcal{G}}^{WS}_{surf}$, we find SSS in Cu and $Cu_{90}Al_{10}$ at energies of 0.594 Ryd (0.33 eV below E_F) and 0.565 Ryd (0.79 eV below E_F) respectively. For the (111)-surface the bulk bands along the Γ–L direction were considered in order to study the $\bar{\Gamma}$-centred SSS; see figure 2 for the case of Cu and $Cu_{90}Al_{10}$. Here SSS were found at energies of 0.6 Ryd (0.25 eV below E_F) and 0.573 Ryd (0.68 eV below E_F) for Cu(111) and the alloy respectively. The disorder induced smearing of the surface states in alloys were estimated from the FWHM of the associated spectral peak, i.e. the integrand in equation (36). In this manner the low-index surfaces, (001), (110), and (111), were studied. No band gaps in the vicinity of the Fermi energy were found in the (001) case, and therefore a further investigation of the surface states was not pursued. The results for the (110) and (111) surfaces of Cu and Cu-based alloys are discussed below.

3.2. (110) and (111) surfaces of Cu, $Cu_{90}Al_{10}$, $Cu_{70}Zn_{30}$, and $Cu_{90}Ge_{10}$

The results for the $\bar{Y}$-centred SSS on the (110) surface and the $\bar{\Gamma}$-centred SSS on the (111) surface are summarized in tables 1 and 2 respectively. A direct comparison between theory and experiment is only possible in Cu and CuAl where these SSS have been observed in angle-resolved photoemission experiments (Asonen *et al* 1982); SSS were not observed in angle-resolved photoemission experiments on CuGe by Bansil *et al* (1984), most likely due to a poor surface quality. We are not aware of any corresponding experiments in CuZn alloys.

Table 1. The calculated binding energies, E_B (theory), and the associated disordered induced smearings (FWHM), δE (theory), for the $\bar{\Gamma}$-centred Shockley state on the (110) surface in Cu and Cu-based alloys; the electron/atom ratios (e/a) for various alloys are given. The experimental values for Cu(110) and $Cu_{90}Al_{10}$(110) are from angle-resolved photoemission experiments of Asonen *et al* (1982); δE (experiment) is estimated from the observed widths of the SSS-feature in Cu and $Cu_{90}Al_{10}$; corresponding data for other alloys is not available. Theoretical and experimental values of shifts in the SSS-binding energy with respect to Cu are given in the fifth and sixth columns, respectively. Units are eV throughout. $\delta E_B^{theory} = (E_B^{alloy} - E_B^{Cu})_{theory}$, $\delta E_B^{expt} = (E_B^{alloy} - E_B^{Cu})_{expt}$.

	e/a	E_B^{theory}	E_B^{expt}	δE_B^{theory}	δE_B^{expt}	δE_{theory}	δE_{expt}
Cu	1.0	0.33	0.39				
$Cu_{90}Al_{10}$	1.2	0.79	0.74	0.46	0.35	0.45	0.36
$Cu_{70}Zn_{30}$	1.3	0.95		0.62		0.34	
$Cu_{90}Ge_{10}$	1.3	1.27		0.94		1.02	

Table 2. As table 1, but for the $\bar{\Gamma}$-centred SSS on the (111) surface. Units are eV throughout. $\delta E_B^{theory} = (E_B^{alloy} - E_B^{Cu})_{theory}$, $\delta E_B^{expt} = (E_B^{alloy} - E_B^{Cu})_{expt}$.

	e/a	E_B^{theory}	E_B^{expt}	δE_B^{theory}	δE_B^{expt}	δE_{theory}	δE_{expt}
Cu	1.0	0.25	0.40				
$Cu_{90}Al_{10}$	1.2	0.68	0.80	0.43	0.40	0.45	0.47
$Cu_{70}Zn_{30}$	1.3	0.85		0.60		0.34	
$Cu_{90}Ge_{10}$	1.3	1.16		0.91		0.99	

Tables 1 and 2 show reasonable agreement between theory and experiment in Cu and $Cu_{90}Al_{10}$. In particular, the theoretically predicted increase in binding energy of the SSS (the fifth column in each table) for both surfaces agrees with the corresponding measured increase in sign; the agreement with regard to the magnitude of the shift appears to be somewhat better for the (111) surface. Note, however, that the concentration of Al in the surface region in the experiments of Asonen *et al* (1982) was estimated to be about 13%; therefore the computed shifts should perhaps be proportionately scaled upwards. The theoretical values for the disordered induced smearing of the SSS in the alloy are in reasonable agreement with the measured increases (the eighth column in each table) in the line widths (FWHM) in the alloy compared with Cu. In general of course a surface state will be broadened in the real system by other mechanisms (e.g. surface imperfections) which are not included in the present theoretical estimate.

With reference to tables 1 and 2, we see that the theoretically predicted binding energy of the SSS increases with increasing electron/atom (e/a) ratios upon adding polyvalent impurities. A substantial solute dependence is nevertheless seen in that while e/a values for $Cu_{70}Zn_{30}$ and $Cu_{90}Ge_{10}$ are the same, the SSS parameters are quite different. Interestingly, the measured position of the SSS in the isoelectronic alloy CuAu is essentially unchanged from Cu, and in CuPd where electrons are depleted from the Fermi energy, the SSS is observed to move to *lower* binding energies with increasing *Pd* content in angle resolved photoemission experiments (Asonen *et al* 1985, Rao *et al* 1984); as noted above, the experimental SSS data in CuZn and CuGe is not available. However, angle-resolved photoemission calculations in Cu-rich CuNi(111)

and CuPd(111) yield an SSS feature at a lower binding energy (Jordan and Durham 1989). Physically, the (110) as well as the (111) SSS arises from bulk sp states in the vicinity of the $L_{2'}$ level. Figures 1 and 2 show that the $L_{2'}$ level is lowered substantially in the alloy, as the average potential in the unit cell becomes more attractive upon adding Al. (A similar effect occurs in CuZn and CuGe.) Therefore, the movement of the Shockley state to a higher binding energy in the alloy is to be expected qualitatively. The magnitude of the SSS shift however is generally less than that of the $L_{2'}$ level. This effect may be understood as being a consequence of the fact that a surface state is less sensitive than the bulk levels to potential changes in the bulk unit cell because the surface is surrounded by bulk atoms on only one side. In $Cu_{90}Al_{10}$, for example, the magnitude of the SSS-shift is only about half as much as that of the $L_{2'}$-level.

4. Discussion and conclusions

The use of non-self-consistent potentials in our work deserves further comment. In principle, the formalism can be developed to obtain a one-site restricted Green function (as opposed to the average Green function, equation (37)) for a single atom placed in the effective KKR-CPA medium in the presence of the surface. The charge density on any site may then be computed, providing a basis for a self-consistent scheme. In actual practice, however, such a procedure will be computationally quite demanding. One important consequence of the fact that we are using the same KKR-CPA scattering potential in all layers is that our model is unable to treat Tamm-type surface states; an extension of the formalism to allow a different potential in at least the topmost surface layer is necessary to obtain such surface states. On the other hand, Shockley states which arise mainly from the mere presence of the surface itself should not be very sensitive to details of the shape of the potential. These considerations provide some justification for assuming that the changes in the Shockley state characteristics upon alloying, our main motivation for this study, may be given reasonably within the framework of our model.

In conclusion, we have developed a Green function matching approach to study Shockley states on an ideal semi-infinite surface of a disordered alloy. Results for the low-index faces of Cu, $Cu_{90}Al_{10}$, $Cu_{70}Zn_{30}$, and $Cu_{90}Ge_{10}$ are presented. Reasonable agreement is found between theoretical predictions and the corresponding angle-resolved photoemission measurements with regard to the characteristic effects of alloying Al (i.e. changes in binding energy, and disorder induced smearing) on the Shockley states of Cu; it would be interesting to obtain experimental Shockley state paramters in CuZn and CuGe alloys. Our calculations indicate that the Shockley state binding energy will generally increase with an increasing electron/atom ratio

Acknowledgments

It is a pleasure to acknowledge important conversations with R S Rao, M Lindroos, and M Pessa, and the technical assistance of E Arola. This project is supported by the US DOE grant ER45223, and a travel grant under the US/Finland program of the NSF, and has benefitted from the allocation of supercomputer time on the ER-Cray at LLNL, and the San Diego Supercomputer Center. Acknowledgement is made to

the donors of the The Petroleum Research Fund, administered by the ACS, for partial support of this research.

References

Asonen H, Barnes C J, Pessa M, Rao R S and Bansil 1985 *Phys. Rev.* B **31** 3245–50
Asonen H, Lindroos M, Pessa M, Prasad R, Rao R S and Bansil A 1982 *Phys. Rev.* B **25** 7075–85
Bansil A 1987 *Electronic Band Structure and its Applications (Springer Lecture Notes in Physics 283)* ed M Yussouff (Berlin: Springer) p 273
Bansil A and Pessa M 1983 *Phys. Scr.* T **4** 52–60
Bansil A, Rao R S, Prasad R, Asonen H and Pessa M 1984 *J. Phys. F: Met. Phys.* **14** 273–9
Berk N F 1975 *Surf. Sci.* **48** 289–303
Bullet D W 1982 *Solid State Commun.* **43** 491–4
Durham P J 1984 *Electronic Structure of Complex Systems* ed P Phariseau and W M Temmerman (New York: Plenum) pp 709–60
Ehrenreich H and Schwartz L M 1976 *Solid State Physics* vol 31 (New York: Academic)
Garcia-Moliner F and Flores F 1979 *Introduction to the Theory of Solid Surfaces* (Cambridge: Cambridge University Press)
Heimann P, Hermann J, Miosga H and Neddermeyer H 1981 *Solid State Commun.* **37** 519–22
Inglesfield J E 1978 *Surf. Sci.* **76** 355–78
—— 1982 *Rep. Prog. Phys.* **45** 223–84
Ishida I, Inoue N and Matsubara T 1976 *Prog. Theor. Phys.* **55** 653–64
Jordan R G and Durham P J 1989 *Alloy Phase Stability (NATO ASI Series B 163)* ed G M Stocks and A Gonis (Amsterdam: Kluwer) pp 35–74
Jordan R G and Sohal G S 1982 *J. Phys. C: Solid State Phys.* **15** L663–7
Pendry J B 1976 *Surf. Sci.* **57** 679–705
Pessa M, Asonen H, Rao R S, Prasad R and Bansil A 1981 *Phys. Rev. Lett.* **47** 1223–6
Prasad R and Bansil A 1982 *Phys. Rev. Lett.* **48** 113–6
Prasad R, Papadopoulus S C and Bansil A 1981 *Phys. Rev.* B **23** 2607–13
Rao R S, A Bansil A, H Asonen and M Pessa 1984 *Phys. Rev.* B **29** 1713–21
Serageldin A Y, Prasad R and Bansil A 1990 *Bull. Am. Phys. Soc.* **35** 296
Stocks G M and Winter H 1984 *Electronic Structure of Complex Systems* ed P Phariseau and W M Temmerman (New York: Plenum) pp 463–85
Velicky B and Kundrnosky J 1977 *Surf. Sci.* **64** 411–24
Wakoh S 1965 *J. Phys. Soc. Japan* **20** 1894–1901
Wysokinski K I, Sobczuk H and Pilat M 1980 *Phys. Status Solidi* b **101** 657–63